Lane Detection Based on Object Segmentation and Piecewise Fitting

Chunyang Mu, Xing Ma*
Institute of Information and Communication Technology, Beifang University of Nationalities,
Yinchuan 750021, China
*Corresponding author, e-mail: maxingsky@126.com

Abstract
        A lane detection algorithm for complex environment was proposed. It was concerned on selecting candidate lane region by object segmentation. Then redundancy edges were extracted by Sobel operator. Furthermore, candidate lane markers were obtained by threshold selection from the edges. Finally lane markers were detected by piecewise fitting. The proposed algorithm was simulated in MATLAB. Experiments showed that lane markers could be detected correctly. Piecewise linear transformation in preprocessing has enhanced performance of detection while the environment was dim. And limited region of interest helps to identification lane in an appropriate region, which have the effect of enhancement in the speed of operation. Feature-based method is usually affected by intensity of image. Several characteristics of roads need to be considered in further for detection more precisely.

Keywords: lane detection, piecewise linear transformation, OTSU object segmentation, threshold selection, piecewise fitting

1. Introduction

        Majority of traffic accidents are caused by error operations or distractions according to the traffic departments' statistics. Accidents caused by these cases could be avoided by continually monitor the position of a car within a lane. The challenging problem is to detect lane boundaries of roads. Now, Europe, America and Japan have thrown themselves into part lane detection system. Some systems, such as the RALPH system, AutoVue system, Start system, AUTORA system and ALVINN system, are representative systems [1, 2].
        Many researches have been developed in this area, however, several complicated nature conditions can decisively degrade the performance of lane detection techniques:
        a) Shadows: trees, buildings and other vehicles project shadows on the road, creating false edges.
        b) Solar position: direct sunlight may saturate the acquired images, or cause specular reflexes.
        c) Climate: natural phenomenal (such as fog, rain or snow) may degrade significantly the quality of the images [3].
        Numerous methods of vision-based lane detection have been proposed in an attempt to robustly detect lanes. They could be categorized in feature-based and model-based method.
        Feature-based method positions the lanes' images by detecting the obvious features, such as lane edges. Hough transform is a most popular method for detecting and locating straight lines in digital images [4], which is not sensitive to noise. However, the computational complexity and storage requirements are the main bottlenecks of the standard Hough transform scheme applied in real-time detection.
        Edge-based methods have been proposed to use straight lines to model lane boundaries. For curved roads, more complex models such as B-Splines, Bezier Splines [5], parabola and hyperbola [6, 7] fitting are often used to provide support. The accuracy of these models is depended on their complexity. Simpler models do not fit lane boundaries accurately though they are more robust to noise than complex models [8].
        For improving the efficient of performance, lower area of a lane image is usually considered as region of interest (ROI) [4]. And this region is further divided into left and right

sub-regions by supposing the width of lane is fixed [1, 9]. Segmenting ROI will reduce the complexity of lane detection.

This research is concerned on selecting an candidate lane region by OTSU object segmentation. Then redundancy potential edge pixels are extracted by Sobel operator. Pixels in these edges are selected by statistic values. Finally, lane markers are obtained by piecewise fitting.

The rest of this paper is organized as follows. Section 2 describes performance of the lane detection algorithm. Several experimental results are presented to support the validity of this method in section 3, and section 4 concludes the paper.

2. Research Method

This method consists of three parts. a) Image preprocessing. It contains color space transformation, and piecewise linear transformation. b) Candidate lane region is obtained by OTSU segmentation and ROI setting. c) Lane markers detection, which is detected by Sobel edge operator firstly. Then candidates are selected by threshold value, and lane markers are piecewise fitted finally. The flow chart of algorithm is shown in Figure 1, which will be described in detail below.
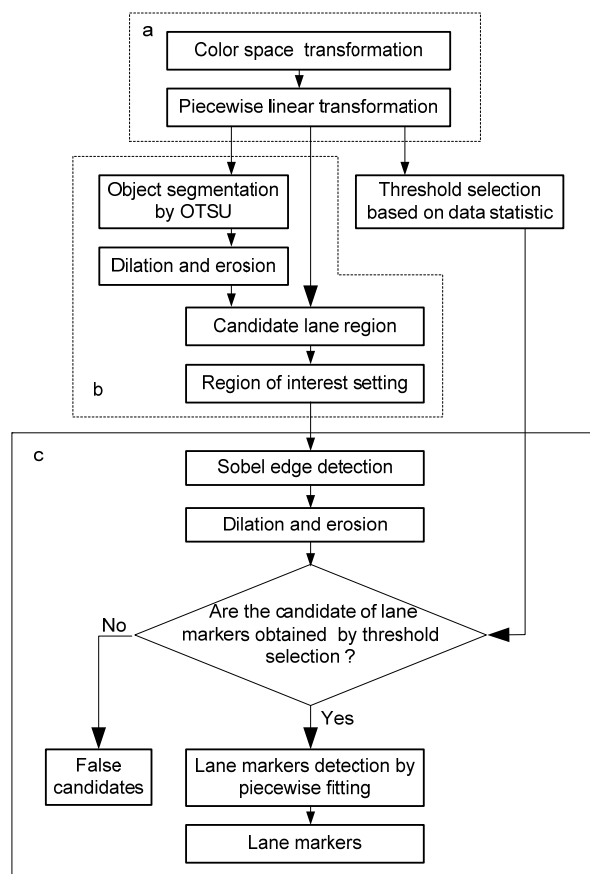
Figure 1. Flow Chart of the Algorithm

2.1. Image Preprocessing
2.1.1. Color Space Transformation

The color of pixels are originally represented in RGB space that is highly correlated [4]. RGB values can be transformed to YCbCr color space. The most visually significant information in the color image is reserved in Y component of image. So Y component of image is used to

detect edges of desired lane. And it also has advantage of saving data storage and reducing computing time.

2.1.2. Piecewise Linear Transformation

It's necessary to transform an image when the enviroment is dim or the image has low contrast. Piecewise linear transformation (PLT) is adopted to adjustment the image contrast. PLT is characterized by $2n$ parameters for n-1 line segments. If the input luminance was $\{x_n,\ n=0,1,\ldots,m\}$ and the output luminance will be $\{y_n,\ n=0,1,\ldots,m\}$, the $(m$-1)th transform functions $T_{m-1}(x)$ will be:

$$T_{m-1}(x) = \frac{(y_m - y_{m-1})}{(x_m - x_{m-1})} \cdot (x - x_{m-1}) + y_{m-1} \tag{1}$$

Segment points are computed based on the histogram data. In this method, we choose the minimum and maximum input gray value as segement points. And they define the segments of the input data. Then each input segment is mapped to an output segment based on a linear transformation for the corresponding segment.

E.g. three segements transformation function $T_0(x)$, $T_1(x)$ are $T_2(x)$ are shown in Figure 2 (a). Given parameters are set as:

$$x_0 = 0,\ y_0 = 0 \tag{2}$$

$$x_1 = MIN,\ y_1 = 0 \tag{3}$$

$$x_2 = MAX,\ y_2 = 255 \tag{4}$$

$$x_3 = 255,\ y_3 = 255 \tag{5}$$

Then the PLT function $T_0(x)$, $T_1(x)$ are $T_2(x)$ are shown in Figure 2(b).

(a) Piecewise linear transformation   (b) Piecewise linear transformatio in this method
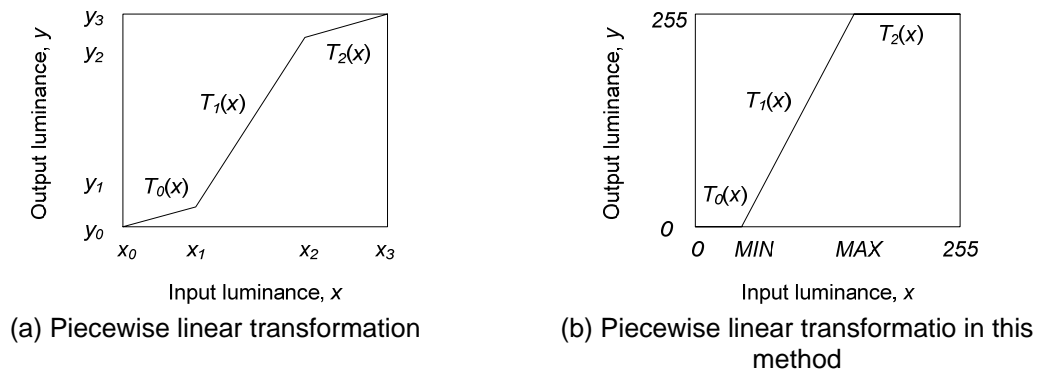
Figure 2. Piecewise Linear Transformation Function

Figure 3 (a) and (b) are an original image and the PTL-based image, respectively. The original image has a low contrast, whose detail cannot see clearly. The PTL-based performent result has been enhanced.

(a) Original image   (b) PLT-based image
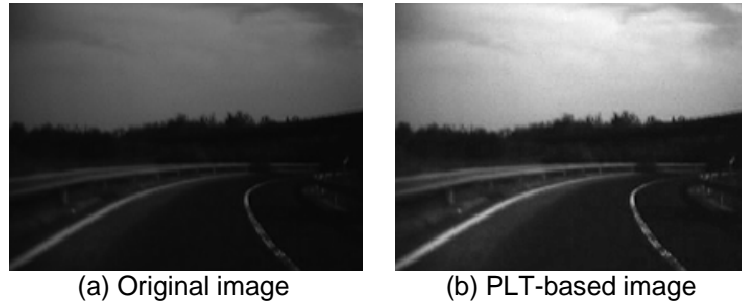
Figure 3. Result of Piecewise Linear Transformation

2.2. Candidate Lane Region
2.2.1. OTSU Segmentation

OTSU segmentation algorithm was proposed by Japanese researcher Nobuyuki Otsu in 1979. The criterion is that maximize the separabilitiy of the resultant classes in gray levels [10]. For extended, m-1 discrete thresholds can divide image into m classes. In this approach, we use two thresholds for separating three classes of lane image.

Let the pixels of a given picture be represented in L gray levels [1, 2, …, L]. The number of pixels level I is denoted by n_i and the total number of pixels by $N= n_1+ n_2 +…+ n_L$. In order to simplify the discussion, the gray-level histogram is normalized and regarded as a probability distribution:

$$p_i = \frac{n_i}{N}, p_i \geq 0, \sum_{i=1}^{L} p_i = 1 \tag{6}$$

We use two thresholds: $1 \leq k_1 < k_2 < L$ for separating three classes, C_0 for [1, … , k_1], C_1 for [k_1+1, …, k_2], and C_2 for [k_2+1, …, L]. Then the probabilities of class occurrence, and the class mean levels are:

$$\omega_0 = P_r(C_0) = \sum_{i=1}^{k_1} p_i = \omega(k_1) \tag{7}$$

$$\omega_1 = P_r(C_1) = \sum_{i=k_1+1}^{k_2} p_i = \omega(k_2) \tag{8}$$

$$\omega_2 = P_r(C_2) = \sum_{i=k_2+1}^{L} p_i = 1 - \omega(k_1) - \omega(k_2) \tag{9}$$

$$\mu_0 = \sum_{i=1}^{k_1} i P_r(i \mid C_0) = \sum_{i=1}^{k_1} i p_i \Big/ \omega_0 = \mu(k_1) \Big/ \omega(k_1) \tag{10}$$

$$\mu_1 = \sum_{i=k_1+1}^{k_2} i P_r(i \mid C_1) = \sum_{i=k_1+1}^{k_2} i p_i \Big/ \omega_1 = \mu(k_2) \Big/ \omega(k_2) \tag{11}$$

$$\mu_2 = \sum_{i=k_2+1}^{L} i P_r(i \mid C_2) = \sum_{i=k_2+1}^{L} i p_i \Big/ \omega_2 = \frac{\mu_T - \mu(k_1) - \mu(k_2)}{1 - \omega(k_1) - \omega(k_2)} \tag{12}$$

Where:

$$\mu(k_1) = \sum_{i=1}^{k_1} ip_i \tag{13}$$

$$\mu(k_2) = \sum_{i=k_1}^{k_2} ip_i \tag{14}$$

And the total mean level of the original picture is μ_T,

$$\mu_T = \mu(L) = \sum_{i=1}^{L} ip_i \tag{15}$$

And there is a relation for choice of k_1 and k_2,

$$\omega_0\mu_0 + \omega_1\mu_1 + \omega_2\mu_2 = \mu_T, \quad \omega_0 + \omega_1 + \omega_2 = 1 \tag{16}$$

The class variances are given by:

$$\sigma_0^2 = \sum_{i=1}^{k_1} (i - \mu_0)^2 P_r(i \mid C_0) = \sum_{i=1}^{k_1} (i - \mu_0)^2 \, p_i \big/ \omega_0 \tag{17}$$

$$\sigma_1^2 = \sum_{i=k_1+1}^{k_2} (i - \mu_1)^2 P_r(i \mid C_1) = \sum_{i=k_1+1}^{k_2} (i - \mu_1)^2 \, p_i \big/ \omega_1 \tag{18}$$

$$\sigma_2^2 = \sum_{i=k_2+1}^{L} (i - \mu_2)^2 P_r(i \mid C_2) = \sum_{i=k_2+1}^{L} (i - \mu_2)^2 \, p_i \big/ \omega_2 \tag{19}$$

The criterion measure σ_B^2 is then a function of two variables and an optimal set of thresholds k_1^* and k_2^*. In order to evaluate the threshold k_1, k_2, the following discriminant criterion measures are used:

$$\lambda = \sigma_B^2 / \sigma_W^2, \kappa = \sigma_T^2 / \sigma_W^2, \eta = \sigma_B^2 / \sigma_T^2 \tag{20}$$

Where:

$$\sigma_W^2 = \omega_0\sigma_o^2 + \omega_1\sigma_1^2 + \omega_2\sigma_2^2 \tag{21}$$

$$\sigma_B^2 = \omega_0(\mu_0 - \mu_T)^2 + \omega_1(\mu_1 - \mu_T)^2 + \omega_2(\mu_2 - \mu_T)^2 \tag{22}$$

And

$$\sigma_T^2 = \sum_{i=1}^{L} (i - \mu_T)^2 p_i \tag{23}$$

An optimal set of thresholds k_1^* and k_2^* is selected by maximizing σ_B^2:

$$\sigma_B^2(k_1^*, k_2^*) = \max_{1 \le k_1 < k_2 < L} \sigma_B^2(k_1, k_2) \tag{24}$$

Results of object segmentation by OTSU are shown in Figure 4-Figure 6. They are two, three and four classifications respectively.

In Figure 4, lane image is represented in binary. In Figure 4(a), the majority road and lane markers are considered as one unit, which is represented in white. While the background is in black. In this result, lane markers are mixed with road. In Figure 4(b) and (c), intensity of the lane markers are higher than road. Therefore most of the lane markers could be detected. But the result of lane detection still have some breakpoint.

In Figure 5, these test scenes are divided into three classifications. And they are represented by three constants, e.g. 0, 0.498 and 1. The classified model is Z.

$$Z = \begin{cases} 0, & C_0, i \in [1, k_1] \\ 0.498, & C_1, i \in [k_1+1, k_2] \\ 1, & C_2, i \in [k_2+1, L] \end{cases} \tag{25}$$

The segmentation results in Figure 5 are more clearly than that in Figure 4. The most prominent of three classifications is that the lane markers, road and background can be divided hierarchically.

Four classifications of lane images are shown in Figure 6. The road is divided into several regions. The more sophisticated classification results are helpless for lane detection in the next steps, but wasting more computation. Above all, we select three classifications of lane image in this method.

(a) Scene 1　　　　　(b) Scene 2　　　　　(c) Scene 3

Figure 4. Classification Results of Two Classes

(a) Scene 1　　　　　(b) Scene 2　　　　　(c) Scene 3
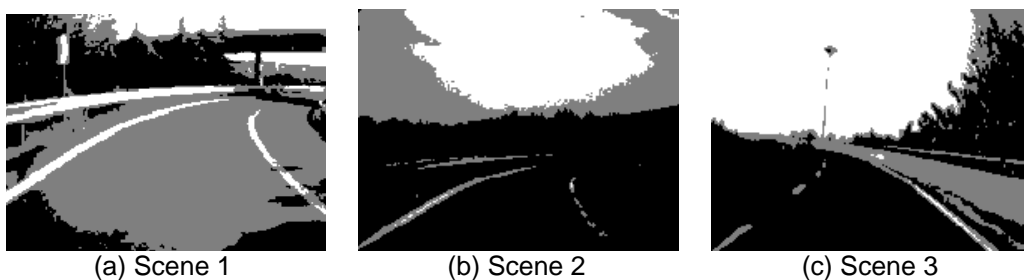
Figure 5. Classification Results of Three Classes

There is some shadow on right side in Figure 5(a). Morphological operate can enchance the performance of classification result disturbed by noisy or shadow. Results of dilation and erosion are shown in Figure 7(a) and (b). The effection of shadow on the right lane marker is almost disapear by dilation and erosion.

(a) Scene 1   (b) Scene 2   (c) Scene 3

Figure 6. Classification Results of Four Classes

(a) Dilation result   (b) Erosion result
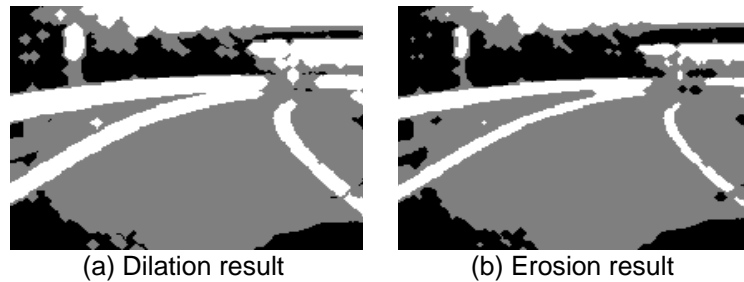
Figure 7. Dilation and Erosion Result

2.2.2. Appropriate Limited Region of Interest

Lane images are captured by a camera which can be situated inside a car near rear view mirror. In upper part of these lane images are sky, buildings, flyovers, trees, street lamps, hills, etc. They have solid liner structure which could be detected out by edge operator. And they might disturb the detection of candidates of lane markers in lower part of images. Thus, it is necessary to set lower area of lane image as ROI. An appropriate limited region of interest (ALROI) is obtained by combined the PLT-based image $b(x,y)$ with ROI and the model $Z(x,y)$, which x and y are coordinate axes in image.

$$ALROI(x, y) = b(x, y) \cdot ROI(x, y) \cdot (Z(x, y) >= Th_a) \qquad (26)$$

Where, Th_a is a threshold for selecting candidate lane region from the PLT-based image. The limited ROI helps to give lane identification in an appropriate region. This process will have the effect of enhancement in the speed of operation.

Candidate lane regions are shown in Figure 8, ALROI covered the majority lane markers, and most of their surrounding environment was masked. But barriers in right side of Figure 8 (c) are left. Because their intensity is similar to lane markers, and they are divided into one unit by OTSU segmentaion.

2.3. Lane markers detection
2.3.1. Sobel Edge Operator

Edges are important features in an image since they represent significant local intensity changes and offer vital clues to separate regions within an object or to identify changes in illumination [4].

(a) Scene 1   (b) Scene 2   (c) Scene 3
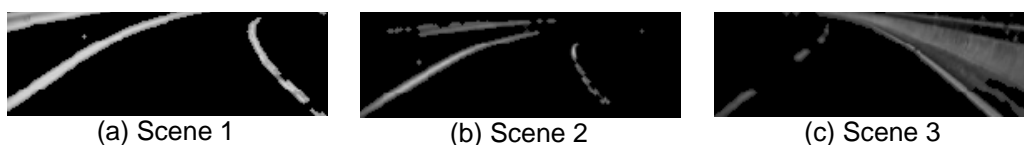
Figure 8. Candidate Lane Region

There are many ways to perform edge detection, Roberts, Canny, Prewitt and so on. We used Sobel edge detection in the limited region. Results are shown in Figure 9.

Figure 9. Result of Sobel Edge Detection

There are still some false edges after Sobel edge detection in an appropriate limited region. These points may disturb lane markers fitting finally. Threshold selection are adopted to resolve it.

2.3.2. Threshold Selection by Data Statistic

Candidate of lane markers are obtained by threshold selection of Sobel edge images. By observing lane image, intensity of lane markers are higher than road in the same scan line. And pixel numbers of lane markers are less. Medium intensity is referenced for statistically generated threshold of every scanline.

$$Th_x = Medium(Region(x,n)) \qquad (27)$$

Where, Th_x is the selection threshold of x-th line. $Region(x,n)$ is an image region from $x-n$ line to $x+n$. $Medium(R)$ is the medium value of region R. And then Th_x is used to distinguish possible lane markers from false edges.

$$CandiLane(x, y) = Edge(x, y) \cdot (ALROI(x, y) > Th_x) \qquad (28)$$

Where, $Edge$ is a binary array after Sobel edge detection, and (x,y) presents the position of a pixel. The distinguish process is concerned on the edge pixels. The intensity of (x,y) in ALROI image is compared with the statistic data Th_x. If the intensity in edge position was larger than Th_x, this edge pixel is truth. Otherwise, it will be considered as a false one, and $CandiLane(x,y)$ will be set 0 accordingly.

Figure 10 shows result of candidate lane edge by threshold selection. Some of the false edge pixels are removed, where it is in bottom of the right side. But there are some still remained due to their intensity is similar to lane markers. Enhancement of performance is needed in further.

Figure 10. Edge Result by Threshold Selection

2.3.3. Piecewise Lane Marker Fitting

Piecewise lane marker fitting is widely used in a roadway under a variety of complicated conditions [3]. In this method, smooth piecewise polynomial functions are used in representing lane markers.

$$Lane(x, y) = \begin{cases} ax^2 + bx + c, & if\ x > x_m \\ dx + e, & if\ x \le x_m \end{cases} \qquad (29)$$

Where x_m represents the border between near and far fields. The linear part of the model is used to fit the near vision field, while the parabolic model fits the far field. This proposed

technique is robust in the presence of noise, shadows, lack of lane painting and change of illumination conditions.

3. Results and Analysis

The lane detection algorithm is simulated in MATLAB. Results of lane detection are pointed out in the gray image with yellow lines.

As shown in Figure 11, we can see that lane markers can be detected correctly although the environment are complicated. The intensity of image in Figure 11(a) and (b) are dim, performance of detection has been enhanced by PLT-based. Moreover there are some shadows cover lane markers in Figure 11(c) and (d). Piecewise lane marker fitting could counteract these disturbs. And one of the lane markers is a dotted line in Figure 11(b) and (e), detection results are also correct.

(a) Scene 1   (b) Scene 2   (c) Scene 3

(d) Scene 4   (e) Scene 5
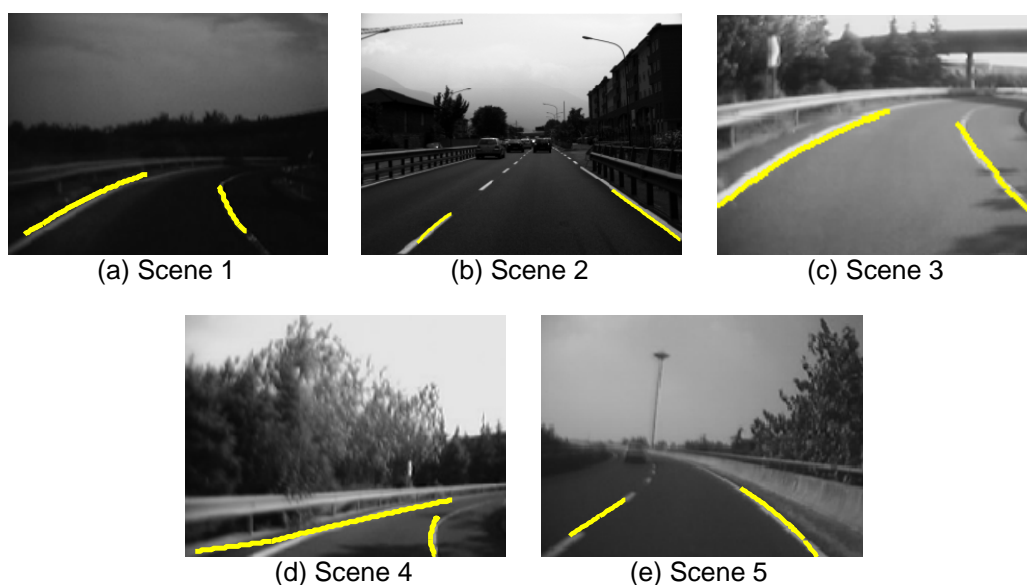
Figure 11. Results of Lane Markers Detection

4. Conclusion

In this paper, a lane marker detection algorithm for sophisticated environment is presented. This study is concerned on selecting candidate lane region by OTSU object segmentation. This is helpful for detection and identification of lane markers in an appropriate region. Experiments shown that lane markers can be detected correctly. For enhanced performance of detection, piecewise linear transformation should be done in preprocessing especially in a dim light environment. And piecewise lane marker fitting is robust in the presence of shadow and lack of lane painting. There are little false lane detection results because feature-based method is usually affected by intensity of image. Several characteristics of road need to be considered for improving the performance of detecting.

Acknowledgements

References

[1] Ronghui Zh, Haiwei W, Xi Zh, Lei W, Tonghai J. Lane detection algorithm at night based-on distribution feature of boundary dots for vehicle active safety. *Information Technology Journal*. 2012; 11(5): 642-646.

[2] Borkar A, Hayes M, Smith MT. A novel lane detection system with efficient ground truth generation. *Intelligent Transportation Systems, IEEE Transactions on*. 2012; 13(1): 365-374.

[3] Jung CR, Kelber CR. *A robust linear-parabolic model for lane following.* IEEE 17th Brazilian Symposium on Computer Graphics and Image Processing. Curitiba. 2004: 72-79.

[4] Chen CY, Chen CH, Dai ZX. An evolutionary computation approach for lane detection and tracking. *Advanced Science Letters*. 2012; 9(1): 342-347.

[5] Aly M. *Real time detection of lane markers in urban streets.* IEEE Intelligent Vehicles Symposium. Eindhoven. 2008: 7-12.

[6] Choi HC, Park JM, Choi WS, Oh SY. Vision-based fusion of robust lane tracking and forward vehicle detection in a real driving environment. *International Journal of Automotive Technology*. 2012; 13(4): 653-669.

[7] Khalifa OO, Assidiq AA M, Hashim AHA. *Vision-based lane detection for autonomous artificial intelligent vehicles.* IEEE International Conference on Semantic Computing. Berkeley. 2009: 636-641.

[8] Javadi MS, Hannan MA, Samad SA, Hussain A. A robust vision-based lane boundaries detection approach for intelligent vehicles. *Information Technology Journal*. 2012; 11(9): 1184-1192.

[9] Sharma S, Shah DJ. A Much Advanced and Efficient Lane Detection Algorithm for Intelligent Highway Safety. *Computer Science & Information Technology.* 2013; 9(1): 51-59.

[10] Otsu N. A threshold selection method from gray-level histograms. Automatica. 1975; 9(1): 62-66.